5

Intraplate earthquakes in North China

MIAN LIU, HUI WANG, JIYANG YE, AND CHENG JIA

Abstract

North China, or geologically the North China Block (NCB), is one of the most active intracontinental seismic regions in the world. More than 100 large (M > 6) earthquakes have occurred here since 23 BC, including the 1556 Huaxian earthquake (M 8.3), the deadliest one in human history with a death toll of 830,000, and the 1976 Tangshan earthquake (M 7.8) which killed ~250,000 people. The cause of active crustal deformation and earthquakes in North China remains uncertain. The NCB is part of the Archean Sino-Korean craton; thermal rejuvenation of the craton during the Mesozoic and early Cenozoic caused widespread extension and volcanism in the eastern part of the NCB. Today, this region is characterized by a thin lithosphere, low seismic velocity in the upper mantle, and a low and flat topography. The western part of the NCB consists of the Ordos Plateau, a relic of the craton with a thick lithosphere and little internal deformation and seismicity, and the surrounding rift zones of concentrated earthquakes. The spatial pattern of the present-day crustal strain rates based on GPS data is comparable to that of the total seismic moment release over the past 2,000 years, but the comparison breaks down when using shorter time windows for seismic moment release. The Chinese catalog shows long-distance roaming of large earthquakes between widespread fault systems, such that no M ≥ 7.0 events ruptured twice on the same fault segment during the past 2,000 years. The roaming of large earthquakes and their long sequences of aftershocks pose serious challenges to the current practice of seismic hazard assessment, and call for a fundamental paradigm shift for studies of intracontinental earthquakes.

Intraplate Earthquakes, ed. Pradeep Talwani. Published by Cambridge University Press.

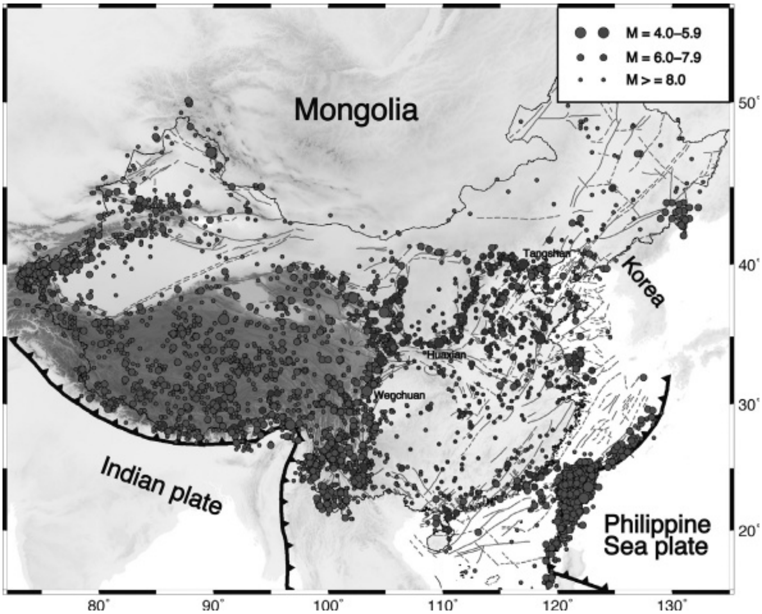

Figure 5.1 Topographic map of China and surrounding regions showing major active faults (thin lines) and seismicity (dots). Blue dots indicate epicenters of historic earthquakes before 1900; red dots indicate earthquakes during 1900–2010 (mostly instrumental records). Inset shows the scales of earthquake magnitudes. The barbed lines represent plate boundary faults. For color version, see Plates section.

5.1 Introduction

In King Jie's 10th year of the Xia Dynasty (1767 BC), an earthquake interrupted the Yi and Lo rivers and damaged houses in the capital city Zhengxuen.

In the second year of King Zhouyou (780 BC), an earthquake dried the Jin, Lo, and Wei rivers, and caused landslides in the Qi mountains.

State Records: Zhou Dynasty

These are some of the earliest written records of earthquakes in China. The Chinese catalog of historic earthquakes goes back ~3000 years, showing more than 1,000 $M \geq 6$ events since 23 BC (Min *et al*., 1995). At least 13 of these events were catastrophic ($M \geq 8$). The 1556 Huaxian earthquake reportedly killed 830,000 people, making it the deadliest earthquake in human history (Min *et al*., 1995). Modern earthquakes in China are intense and widespread. The 1976 Tangshan earthquake (Mw 7.8) killed ~242,000 people and injured millions (Chen *et al*., 1988).

Most of these earthquakes occurred within the continental interior (Figure 5.1). In western China (approximately west of 105° E), historic earthquake records are sparse, but instrumentally recorded seismicity is intense. These earthquakes are directly related to the ongoing Indo-Asian continental collision; most of them are concentrated along the roughly E–W-trending fault systems resulting from the collision.

Seismicity in eastern China is weak today relative to western China, but the long historic records in eastern China show abundant large earthquakes, especially in the North China Block (NCB) (Figure 5.1). Here the fault systems are more complex: in the North China Plain and the coastal regions, the fault systems are mostly NE and NEE trending, owing their origin to subduction of the Pacific plate under the Eurasian plate (Deng *et al.*, 2002; Zhang *et al.*, 2003); further to the west, seismicity is concentrated in the rift fault zones around the Ordos Block.

The NCB is a geological province including the Ordos Plateau and the surrounding rift systems, the North China Plain, and the coastal regions. The cause of earthquakes in the NCB is uncertain. These earthquakes are clearly intraplate events, because the NCB is located in the interior of the Eurasian plate, within the Archean Sino-Korean craton, and thousands of kilometers away from plate boundaries. North China, being the cradle of the Chinese civilization, has the most complete historic records of earthquakes. Today, North China is one of the most densely populated regions in China with vital economic and cultural centers; hence, understanding earthquake hazards here is of great importance. In past decades, intensive geological and geophysical studies in North China have greatly refined the geological history and earth structure, and extensive Global Positioning Systems (GPS) measurements have delineated crustal kinematics. In this chapter, we briefly summarize the tectonic background of the North China region, discuss the main features of active tectonics, and describe historic and instrumentally recorded earthquakes. We highlight the complex spatiotemporal patterns of large earthquakes in North China, and discuss their implications for earthquake hazard assessment in North China and other mid-continents.

5.2 Tectonic background

The geologically defined North China Block is part of the Archean Sino-Korean craton; in China it is also referred to as the North China Craton (NCC). From west to east, the NCB includes the Ordos Plateau, the North China Plain, and the coastal regions (Figure 5.2). The Ordos Plateau is a relic of the NCC, with thick lithosphere and little internal deformation through the Cenozoic, hence is also referred to as the Ordos Block. Its margins are bounded by a system of rifts developed in the late Cenozoic, perhaps as a consequence of the Indo-Asian collision (Xu *et al.*, 1993; Zhang *et al.*, 1998). These rifts include the Weihe rift and the Shanxi rift on the southern and eastern margins of the Ordos Plateau, respectively. These rifts are structurally connected and perhaps formed together; in China they are sometimes collectively referred to as the Fenwei rift system. This is a major seismic zone in North China (Figure 5.2).

The North China Plain and the coastal regions are the part of the Sino-Korean craton where the cratonic root was destroyed by thermal rejuvenation in the Mesozoic; the process produced widespread extension and volcanism during the late Mesozoic and early

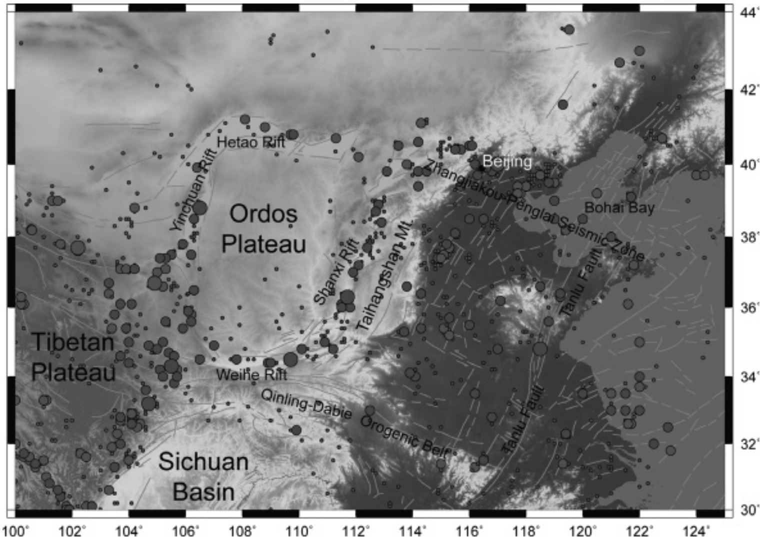

Figure 5.2 Topographic relief (colored background), faults (orange lines), and seismicity (dots for epicenters) for North China. Blue dots: historic earthquakes; red dots: instrumentally recorded earthquakes. For color version, see Plates section.

Cenozoic. Today, these regions are marked by flat, low-elevation (~50–200 m) and thin lithosphere (~60 km in places), and the upper crust includes thick Quaternary sediments covering widespread extensional basins. The fault systems are complex and widespread. The boundary between the North China Plain and the coastal regions is the northeast-trending Tanlu fault (Figure 5.2), a major strike-slip fault system developed during the Mesozoic collision between the North and South China blocks, but with little slip through the Cenozoic (Li, 1994; Yin and Nie, 1996; Wang *et al.*, 2011).

The southern boundary of the North China Block is the east-trending, late Triassic Qinling–Dabie orogenic belt created by the collision between the North and South China blocks (Figure 5.2); the northern boundary is the Hetao rift valley along the northern rim of the Ordos Plateau, and the Yanshan–Yinshan mountain belts further to the east. Along the southwestern margin of the North China Block, the Ordos Plateau encounters the northeastern corner of the laterally expanding Tibetan Plateau, forming a fold-and-thrust belt in the late Cenozoic.

The topographic boundary between the high-standing western part of the North China Block and the low-altitude North China Plain is abrupt along the eastern flank of the Taihangshan mountain ranges (Figure 5.2). This boundary is also marked by the largest gradients of gravity in east Asia, corresponding to large gradients of crustal and lithospheric thicknesses (Ma, 1989). The upper mantle under the North China Plain and the coastal regions is characterized by low seismic velocity structures, which may be related to mantle flow above the subducted Pacific plate (Liu *et al.*, 2004; Huang and Zhao, 2006).

5.2.1 Geological history

Much of the basement of the North China Block belongs to the Sino-Korean craton, which includes some of the oldest rocks on Earth (Liu *et al*., 1992). During the Late Archean to Paleoproterozoic, the Western Block, which includes the Ordos Block, collided with the Eastern Block, forming the Trans-North China Orogen, which includes the basement of today's Shanxi graben and the Taihangshan mountains (Zhao *et al*., 2005; Zhai and Santosh, 2011). Since then the North China basement has been a coherent craton and remained tectonically stable until the end of the Paleozoic. Geological evidence indicates that the lithosphere under eastern North China was more than 180 km thick in the early Mesozoic (Griffin *et al*., 1998; Xu *et al*., 2003).

During the Triassic to mid-Jurassic, the North China Block collided with the South China Block, resulting in the Qinling–Dabie orogenic belt with ultra-high-pressure metamorphism. The collision modified the crustal and lithospheric architecture of the North China Block, producing thick-skinned crustal thrusts in its southeastern part (Li, 1994), forming major faults, such as the Tanlu fault, which cut across the entire craton. This collision probably also initiated the thinning of the North China lithosphere (Menzies *et al*., 2007).

Most of the lithospheric thinning in North China occurred during the late Mesozoic to early Cenozoic, accompanied by widespread extension and volcanism (Zhu *et al*., 2012b). Petrological and geochemical probing using the upper mantle xenolith indicates that the lithosphere was thinned to ~80 km over much of the eastern NCB and less than 60 km thickness in some places (Menzies and Xu, 1988; Xu *et al*., 2003). This is consistent with seismic data (Chen *et al*., 2009). The cause of the removal of the cratonic root under North China remains poorly known (Zhu *et al*., 2012a). It may have resulted from the Mesozoic collision between the North and South China blocks, which led to delamination or thermal erosion of a thickened and weakened lithosphere (Xu, 2001; Bryant *et al*., 2004), or it may be related to the ocean-ward retreat of the western Pacific plate, which induced mantle upwelling under North China. The Cenozoic tectonism in North China may also be linked to indentation of India with Eurasia and the induced lateral mantle flow (Liu *et al*., 2004).

5.2.2 Lithospheric structure

Seismic imaging shows that the eastern North China Block is underlain by broad low-velocity mantle structures (Figure 5.3). These low-velocity structures are limited to the upper mantle; at ~660 km depth flat subducting slabs, shown as a high-velocity layer, can be traced to the subduction zone of the Pacific plate along the eastern margins of the Eurasian plate (Huang and Zhao, 2006). The western end of the stagnant slabs extends ~1500 km inland from the active trench in the western Pacific, and can be correlated with the prominent surface topographic change between the high-standing Ordos Plateau and the Taihangshan mountains in the west, and the lowland of the North China Plain and

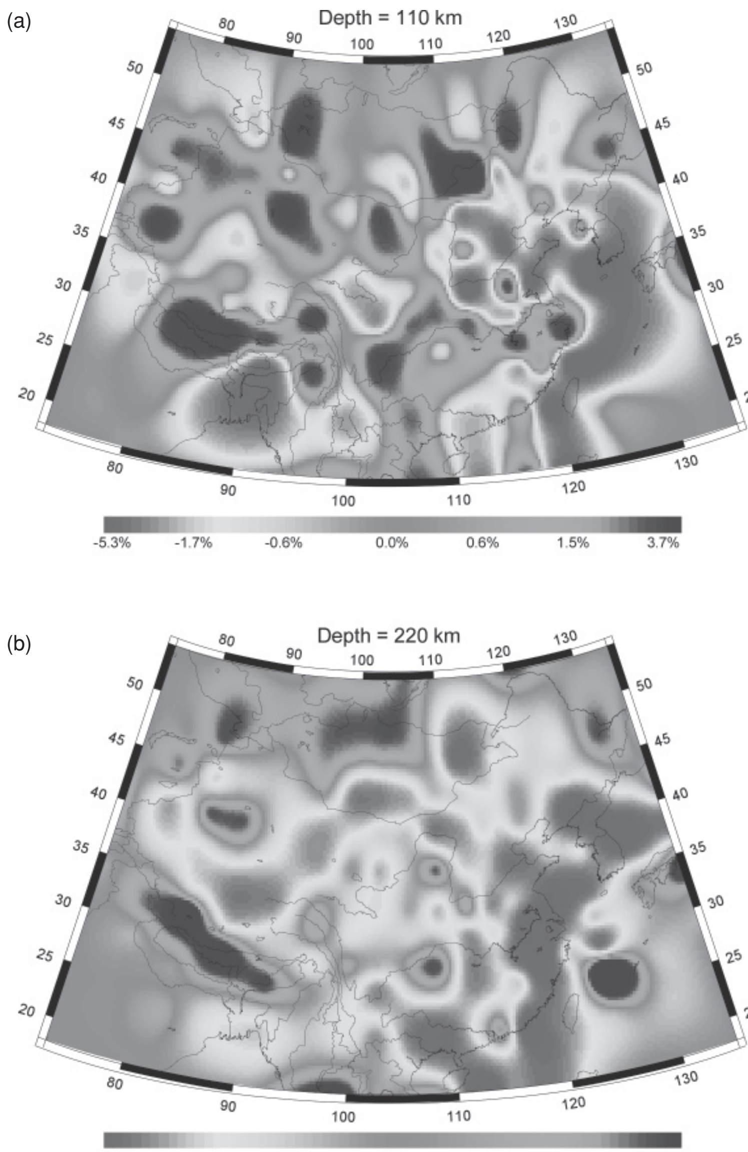

Figure 5.3 P-wave travel time seismic tomography of China and the surrounding regions. (a) P-wave velocity perturbation at 110 km depth. (b) P-wave velocity perturbation at 220 km depth. From Liu *et al*. (2004). For color version, see Plates section.

coastal regions in the east. Hence, the low-velocity mantle structures under North China may be a horizontally expanded “mantle wedge” above both the active subducting slab in the western Pacific and the stagnant slabs beneath much of the North China Plain (Huang and Zhao, 2006). This broad mantle wedge probably resulted from seaward retreat of the western Pacific trench and the sinking of the Mesozoic and Cenozoic slabs now trapped at the 660 km transition zone. Convection in this mantle wedge could have contributed to the Cenozoic lithospheric thinning, volcanism, and associated extensional basins in the eastern NCB (Liu *et al*., 2004; Zhu *et al*., 2009).

Accordingly, the lithosphere under the eastern NCB is abnormally thin, in some places reaching ~60–80 km (Chen *et al*., 2009; Huang *et al*., 2009). It thickens westward, reaching more than 200 km under the Ordos Plateau (Chen *et al*., 2009). The thickening occurs abruptly along the foothills of the Taihangshan mountains, correlating to the western edge of the stagnant subducting slabs. Whereas the western part of the NCB avoided thermal thinning for the most part, the lithosphere under the rift systems around the Ordos Block may be thinned to 80 km (Chen *et al*., 2009).

The variation of crustal thickness generally mimics that of the lithosphere. It is more than 40 km thick in the western NCB, and thins to 32–26 km in the eastern NCB (Ma, 1989). The Ordos Plateau has a thin Cenozoic cover; in many places the Mesozoic strata, which are a few kilometers thick, are exposed. These strata are flat-lying except near the margins of the Ordos Plateau, indicating the tectonic stability of the western NCB since at least the Mesozoic time (Zhang *et al*., 2007). In contrast, the eastern NCB is covered by thick Cenozoic sediments, on top of widespread extensional basins, the largest one being the basin system centered around Bohai Bay (Allen *et al*., 1998; Li *et al*., 2012) (Figure 5.2). In these regions the upper crust is crosscut by a complex system of listric normal faults associated with these extensional basins; they change to strike-slip faults in the middle–lower crust where most of the destructive large earthquakes in the NCB initiated (Xu *et al*., 2002b).

5.2.3 Major seismogenic faults

Seismicity in the western NCB is concentrated within the circum-Ordos rift systems (Figure 5.2). These rifts developed mainly in the Neogene, related to the Indo-Asian collision and the northeastern expansion of the Tibetan Plateau (Ye *et al*., 1987; Zhang *et al*., 1998). Along the northwestern edge of the Ordos Block is the Yinchuan rift, which connects with the Hetao rift along the northern side of the Ordos. On the southern side of the Ordos Block is the Weihe rift, which produced the deadly 1556 Huaxian earthquake. Along the southeastern edge of the Ordos Block, the Weihe rift connects with the northeast-trending Shanxi rift, which is a dextral shear extension zone consisting of more than 10 discontinuously distributed fault-depression basins controlled by normal strike-slip faults or normal faults (Deng *et al*., 2003). Together, these two rifts have hosted more than 36 large ($M > 6.5$) earthquakes since 1303 (Liu *et al*., 2007). Seismicity within the Ordos Plateau is minor, similar to seismicity in other stable cratons (Mooney *et al*., 2012).

In the eastern NCB the most prominent fault is the Tanlu fault system, which was developed during the Mesozoic collision between the South and North China blocks (Li, 1994; Yin and Nie, 1996). Its Cenozoic development may be related to the opening of Bohai Bay during the Paleogene back-arc extension (Ren *et al*., 2002). GPS surveys show that the fault is extensional, accommodating east–west extension (Shen *et al*., 2000). Although the present-day slip rate is less than 1 mm/yr (Wang *et al.*, 2011), its rupture in 1668 caused the Ms 8.5 Tancheng earthquake.

The northern margin of the North China Plain is bounded by the Zhangjiakou–Penglai fault, a complex, NW–SE-trending fault system that is up to a few tens of kilometers wide as it extends to the coastal regions (Figure 5.2). Its intersections with a system of NE-trending faults in the North China Plain, including the Tanlu fault, are the source regions of a number of destructive earthquakes.

The North China Plain, between the Shanxi rift and the Tanlu fault, has a complex system of faults, mainly NNE-trending, which are covered by thick Quaternary sediments, with little or no surface traces (Deng *et al.*, 2003). Some of these faults, including the Xingtai–Hejian–Tangshan fault zone, were recognized only after the destructive 1966 Xingtai earthquake (M 7.2) and the 1996 Tangshan earthquake (M 7.8).

5.3 Active tectonics and crustal kinematics

North China, with its dense population and intense seismicity, is one of the best studied regions in China. A "Map of Active Tectonics of China," at a scale of 1:4 million, identified more than 200 active tectonic zones (Deng *et al.*, 2003). This map delineates the active tectonic belts of China that bound relatively aseismic blocks.

The GPS network in North China was established in 1992; it was significantly improved with the establishment of the Crustal Motion Observation Network of China (CMONOC) in 1998. About 300 CMONOC survey mode GPS stations are located in North China, covering effectively all the known regional active faults (Figure 5.4). Shen *et al.* (2000) found that regional deformation in North China is dominated by left lateral slip (~2 mm/yr) across the east-southeast-trending Zhangjiakou–Penglai seismic zone and extension (~4 mm/yr) across the north-northeast-trending Shanxi rift, which could be comparable with the ~1.0 mm/yr estimated from seismic moment data (Wesnousky *et al.*, 1984) and 0.5–1.6 mm/yr averaged over the Late Pliocene–Quaternary time (Zhang *et al.*, 1998). However, using a more complete dataset, He *et al.* (2003) found no clear signal of extension across the Shanxi rift; they attributed the discrepancy with geological extension rate to time-dependent extensional processes.

5.4 Strain rates and seismicity

Using the GPS data from China's CMONOC network, Liu and Yang (2005) calculated the scalar strain rates, defined as $\dot{\mathrm{E}} = (\dot{\varepsilon}_{\phi\phi}\dot{\varepsilon}_{\phi\phi} + \dot{\varepsilon}_{\lambda\lambda}\dot{\varepsilon}_{\lambda\lambda} + 2\dot{\varepsilon}_{\phi\lambda}\dot{\varepsilon}_{\phi\lambda})^{1/2}$, where ϕ and λ are longitude and latitude, respectively, in North China (Figure 5.5). The higher strain rates are found in the North China Plain and around the Ordos Block. The Shanxi rift system, which has had many large earthquakes in the past 2,000 years (Figure 5.1), surprisingly shows relatively low strain rates. This is consistent with the GPS results (He *et al.*, 2003), and may be related to the seismic quiescence within the Shanxi rift in the past 300 years (Liu *et al.*, 2007, 2011).

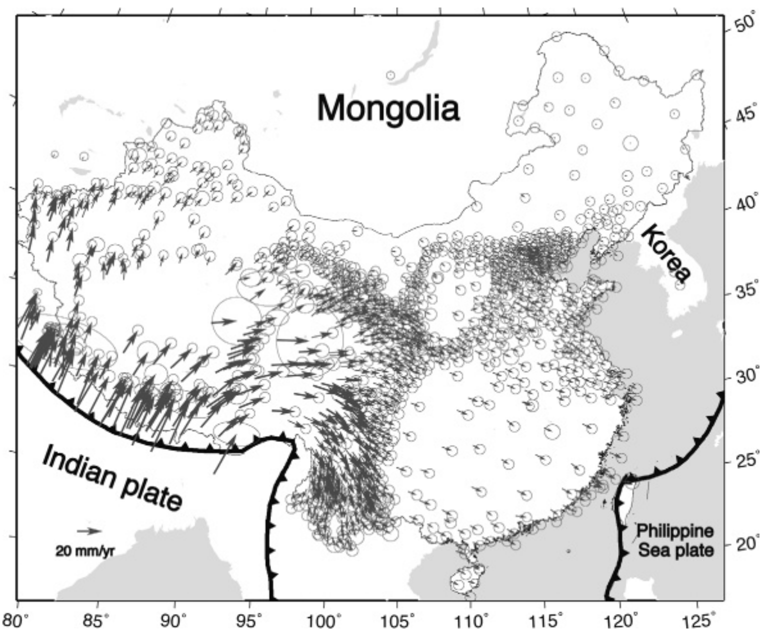

Figure 5.4 GPS site velocities in mainland China relative to stable Eurasia. Data from Zhang and Gan (2008). Error ellipses represent the 95% confidence level.

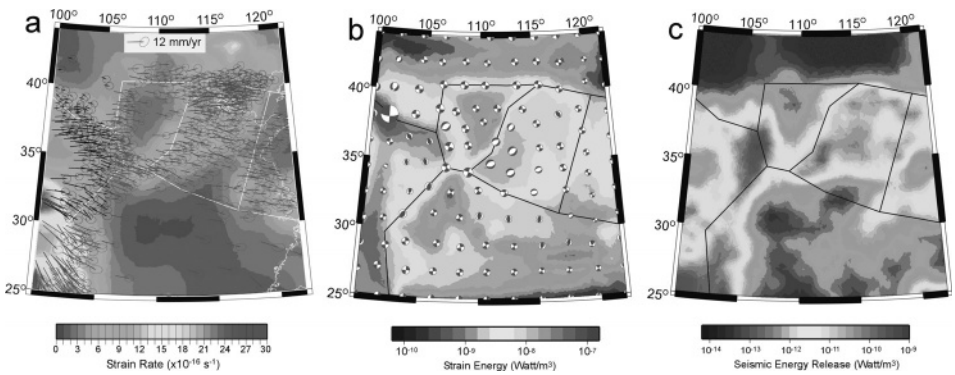

Figure 5.5 (a) GPS velocity (relative to stable Eurasia) and strain rates (background). (b) Predicted long-term strain energy (background) and stress states represented in stereographic lower-hemisphere projections. (c) Seismic strain energy released in the past ~2,000 years. Modified from Liu and Yang (2005). For color version, see Plates section.

Using the velocity boundary conditions extrapolated from the GPS data, Liu and Yang (2005) developed a 3D finite element model to calculate the long-term distribution of strain rate and strain energy (the product of scalar strain rate and stress) in North China (Figure 5.5b). The spatial pattern of strain energy is comparable with seismic moment release in the past ~2,000 years, estimated using the Chinese historic catalog (Figure 5.5c).

This indicates that the intense seismicity recorded in North China in the past 2,000 years is a close reflection of the long-term strain energy accumulation and release. One major mismatch is along the northern margin of the Ordos Plateau, where the relatively low seismic moment release contradicts the high long-term strain energy predicted by the model. A similar discrepancy was found by Wang *et al*. (2011), who derived the slip rates on major fault zones in continental China and compared the rates of moment accumulation with that released by recorded earthquakes. This inconsistency between low moment release and high strain energy may indicate a surplus of moment along the northern boundary of the NCB.

In general, however, seismic moment release, which is limited by the incomplete earthquake catalog, is incompatible with strain rates derived from GPS measurements. To illustrate the bias of inferred spatiotemporal patterns of seismicity from the incomplete earthquake record, Figure 5.6 plots the spatial distribution of moment release within a 250-year time window in North China in the past 750 years, a period of the most complete earthquake record in the Chinese catalog. Note that the spatial pattern of moment release within each time window differs from all others, and none of them is comparable with the strain rates derived from the GPS data (Figure 5.5a). These results highlight the complex spatiotemporal patterns of intracontinental earthquakes, and the problem of long recurrence time and short and incomplete records. The apparent consistency between the total seismic moment release and the strain rates based on GPS data in North China is an exception rather than the norm; this can be largely attributed to the more than 2,000-years of earthquake records in North China. The catalog is much shorter in other mid-continents. In the Central and Eastern United States, the historic catalog only extends for 200 years or so, therefore the spatial pattern of seismicity from these records may not be a reliable indicator for the long-term seismicity or what seismic activity will look like in the next few hundred years.

5.5 Seismicity

North China has the most complete earthquake records in China because it is the cradle of the Chinese civilization. The ancient Chinese regarded earthquakes and other natural hazards as the wrath of heaven; these events were faithfully recorded by the government. The earliest written record of earthquakes in North China may be traced back to the twenty-third century BC (Gu *et al*., 1983); however, the record is likely incomplete, and most of the early records are sketchy. Recent paleoearthquake studies, mainly through trenching, have extended the earthquake history in many sites (Xu *et al*., 2002a).

5.5.1 Paleoseismicity

Most paleoseismic studies in North China have been focused on the rift zones around the Ordos Plateau. Along the northern edge of the Ordos Block, Ran *et al*. (2003a) identified 62 paleo-earthquakes in the late Quaternary, 33 of which occurred in the Holocene. They

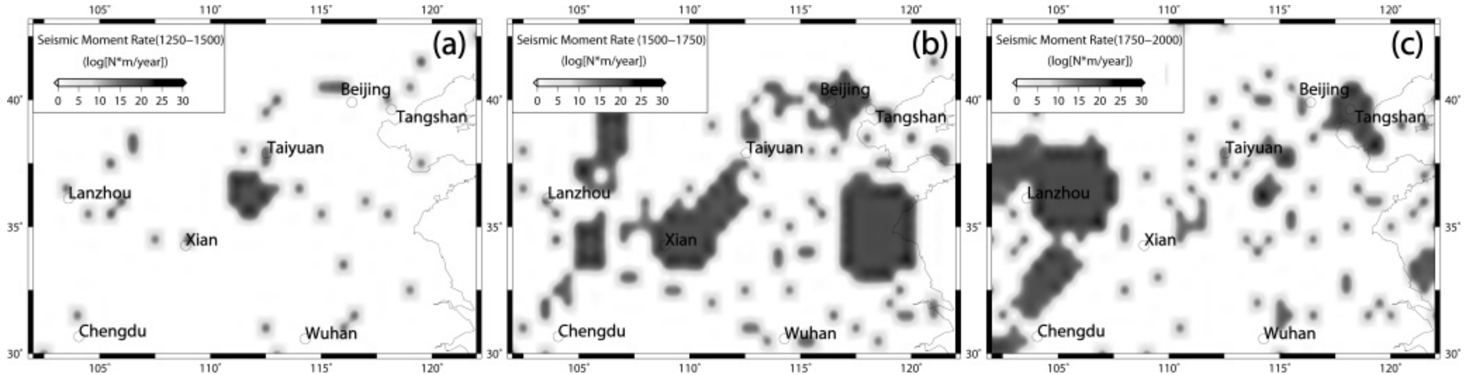

Figure 5.6 Spatial patterns of seismic moment release rate in North China averaged over different time windows: (a) 1250–1500; (b) 1500–1750; (c) 1750–2000. Moment is in Newton meter.

also found that the recurrence intervals of major earthquakes differ for individual fault segments, individual faults, and composite fault zones. One of the major faults is the 220 km long Daqingshan normal fault zone, which was initiated in the Eocene, with a total slip of more than 2.4 km since the Quaternary. Seven major paleoseismic events have occurred since 19 ka BP (thousands of years before present), with an average recurrence interval of ~2,000 ± 432 years (Ran *et al.*, 2003b).

Along the Yinchuan rift valley on the northwestern edge of the Ordos Plateau, Deng and Liao (1996) identified four large earthquakes (M 8.0) at around 8,400, 5,700, 2,600, and 256 years before present, with a recurrence interval of 2,300–3,000 years. Within the Weihe rift valley, where the Huaxian earthquake (M 8.0) occurred in 1556 (see below), trenching unveiled two more events around 2,715 and 5,610 years before present (Xu *et al.*, 1988b).

The Shanxi rift zone on the eastern side of Ordos has produced many large earthquakes (Figure 5.2). In its southern part where an M 8 event occurred in 1303 (see below), two more events occurred around 3,336–2,269 and 5,618–4,504 years before present (Bi *et al.*, 2011). On one of the faults in the central segment of the Shanxi rift, trenching shows three events around 3.06–3.53, ~5.32, and ~8.36 ka BP; the coseismic vertical slips of these events were 1.5–4.7 m, indicating magnitudes to be M 7.0 or above (Guo *et al.*, 2012). On the western branch of the northern segment of the Shanxi rift, four events occurred around 2.52, 5.68, 6.76–10.82, and 12.34 ka BP (Xie *et al.*, 2003). Trenching of various fault strands of the Shanxi rift system has revealed many other events, with recurrence times typically of a few thousand years.

Paleoseismic studies in the North China Plain, which is covered by thick Quaternary sediments, are less extensive and have been focused on where large historic earthquakes occurred. On the Tanlu fault, where the Ms 8.5 Tancheng earthquake occurred in 1668 (see below), trenching uncovered at least three more events around 3,500, 5,000–7,000, and ~10,000 years before present (Lin and Gao, 1987). The fault system bounding the northern side of the North China Block hosted the 1679 Sanhe earthquake (M 8.0); trenching studies there suggested three previous events around 10.85–9.71 ka BP, 7.390–6.68 ka BP, and 5.416–2.233 ka BP (Xu and Deng, 1996).

5.5.2 Large historic events

The Chinese catalog of historic earthquakes shows 49 large (M ≥ 6.5) events in North China since 1303 (Min *et al.*, 1995), including five catastrophic (M ≥ 8.0) events, which are described here.

1303 Hongdong earthquake (M 8.0)

The Great Hongdong earthquake occurred on September 17, 1303, near the Hongdong County within the Shanxi rift zone. The epicenter is estimated to be around 111.7° E, 36.3° N. The damaged area was about 500 km long and 250 km wide; the intensity reached

XI around the epicenter. Within the 44 km long and 18 km wide epicentral region all buildings were wiped out.

Earthquake damage was reported in 45 counties of three provinces. The death toll varies among different records, ranging from ~270,000 to ~470,000 (Yao *et al.*, 1984; Min *et al.*, 1995). Damage was widespread and extended to more than 250 km from the epicentral region. More than 100,000 houses and public buildings (mainly temples) were destroyed; fissures and sand blows were recorded in many places.

Since the 1960s, the site(s) of the Hongdong earthquake and the historic records have been studied by various groups (Su *et al.*, 2003). The 60 km long Huoshan fault was identified as the hosting fault (Xu and Deng, 1990). Xu and Deng (1990) estimated the surface rupture of the earthquake to be 45 km long with dextral and normal slips. They concluded that the maximum strike-slip displacement was about 10 m; the maximum normal slip was about 3–5 m.

1556 Huaxian earthquake (M 8.3)

The M 8.3 Huaxian earthquake occurred in the middle of the night of January 23, 1556, within the Weihe rift. The annals of the Ming Dynasty describe it this way: "Shanxi, Shannxi, and Henan provinces shook simultaneously with thundering sound. Damage was especially severe in Weinan, Huaxian, Zhouyi, Shanyuan, and Puzhou counties. Ground cracked, water gushed out, houses sank into ground, and hills were created suddenly. Rivers flooded, mountains collapsed, the death toll with named victims reached over 830,000; unnamed victims were countless." Landslide, flooding, famine, the bitter weather, and plague all contributed to the stunning death toll. This is the deadliest earthquake in human history.

Damage was reported in 101 counties in Shanxi province and four neighboring provinces, over a region of ~280,000 km^2. The maximum intensity reached XI in the epicentral region of 2,700 km^2. Historic records include detailed descriptions of surface ruptures, liquefactions, terrain changes, and flooding of the Yellow River and the Weihe River (Li, 1981).

The rupture was on the transtensional Huashan fault; the ruptured surface trace was about 200 km (Huan *et al.*, 2003). The average displacement was about 4 m (Xu and Deng, 1996). Within the epicentral region, broad subsidence occurred north of the fault and uplift south of the fault. The vertical offset reaches 10 m in Huaxian County.

1668 Tancheng earthquake (M 8.5)

The M 8.5 Tancheng earthquake occurred in the evening of July 25, 1668, on the Tanlu fault near Tancheng County (34.8° N, 118.5° E), Shandong Province. More than 50,000 people were killed, and damage was reported in 150 counties (Ma and Zhong, 2009).

This earthquake was recorded in more than 500 historic books and monuments. The annals of the Tancheng County described the earthquake as follows: "In the evening, a piercing sound suddenly came from the northwestern direction. The houses and trees moved up and down twice or three times, and then shook from side to side. The city walls, residential houses, and temples all collapsed.” Near the epicenter the damage was complete, no building survived in a region of hundreds of square kilometers. The maximum intensity reached XII. Liquefaction was widespread; one village with thousands of families sank into the ground. The earthquake was followed by half a dozen large (M 6–7) aftershocks. The earthquake also caused a breach in the banks of the Yellow River, flooding a large area.

The Tancheng earthquake ruptured five segments of the Tanlu fault, with a total rupture length of 130 km. The maximum coseismic horizontal slip was about 10 m and vertical slip was about 3 m (Wang and Geng, 1996).

1679 Sanhe earthquake (M 8.0)

The M 8 Sanhe earthquake occurred on September 2, 1679, 40 km northeast of Beijing. The epicentral region includes the Sanhe and Pinggu counties, Hebei Province. The intensity reached XI in these two counties.

The Annals of the Sanhe County described the event: “. . . the earthquake occurred in the evening, with ground shaking from northwest to southeast. People couldn’t stand on the ground, which moved like a boat tossed in a stormy sea. Nearly all houses collapsed. The ground cracked everywhere with black water swelling up for more than a month.” The official death toll was more than 10,000 in Pinggu County, and 2,677 in Sanhe County. In Beijing, 485 people were killed, many buildings, including palaces in the Forbidden City and the city walls, cracked. The emperor Kangxi and the royal family stayed in tents as a precaution.

The surface rupture was estimated to be about 56 km (Xu *et al*., 2002b), and the average coseismic vertical displacement was 1.4–3.16 m based on various drilling cores (Ran *et al*., 1997; Jiang *et al*., 2000). The hosting fault is part of the complex Zhangjiakou–Penglai fault system bounding the northern margin of the North China Block.

1695 Linfen earthquake (M 7.5–8.0)

On May 18, 1695, an M 7.5–8.0 earthquake occurred in the Linfen basin in the southern part of the Shanxi rift system (Wu *et al*., 1988). According to the Annals of Linfen County, the earthquake occurred around 8:00 p.m. local time, with thundering sounds. In the epicentral region, 70–80% of buildings collapsed. Damage was reported in 125 counties of Shanxi and the neighboring provinces. The death toll varies among different records; it was ~56,200 in an official study conducted in 1875, while a Yuan Dynasty monument stated that 176,365 people lost their lives in this earthquake.

The epicenter of this earthquake is near that of the 1303 Hongdong earthquake, but on a different fault. The Linfen earthquake ruptured along a northwest-trending fault that cut the northeast-trending fault for the 1303 Hongdong earthquake. The rupture length of the Linfen earthquake was about 70 km, with a high dip angle and sinistral slip (Cheng *et al*., 1995; Hu *et al*., 2002).

5.5.3 Large instrumentally recorded earthquake

Several earthquakes larger than M 7.0 in the North China Plain have been recorded by instruments since 1960 (Figure 5.2). The most devastating ones include the Xingtai, Haicheng, and Tangshan earthquakes.

The 1966 Xingtai earthquake (Ms 7.2)

Between March 8 and 29, 1966, a cluster of five earthquakes larger than M 6.0 occurred in the Xingtai region of the Hebei Province. The largest one was an Ms 7.2 event which occurred on March 22; the maximum intensity reached X in the epicentral region. These earthquakes destroyed more than 5 million buildings, killed 8,064 people and injured ∼38,000 (Seismological Bureau of Hebei Province, 1986).

The earthquake cluster occurred on a NNE-trending right-lateral fault along the Sulu graben (Chung and Cipar, 1983; Xu *et al.*, 1988a). The rupture length is about 50 km, and the maximum right-lateral strike-slip displacement was ∼1.0 m (The Geodetic Survey Brigade for Earthquake Research, 1975). The focal depths of these events range from 9 to 25 km (Chen *et al.*, 1975), consistent with the depths of aftershocks.

The 1975 Haicheng earthquake (Ms 7.3)

The 1975 Haicheng earthquake occurred on February 4 in the Haicheng region, Northeastern China (122.83° E, 40.70° N), on the northwest-trending Jingzhou–Haicheng fault. The focal depth is 16–21 km, with a surface rupture of ∼50 km length. The maximum left-lateral slip is 0.55 m (Jones *et al.*, 1982; Zhu and Wu, 1982).

The Haicheng earthquake's maximum intensity reached IX, yet the human casualties, with 1,328 killed and 16,980 injured, were much fewer than usual thanks to a successful prediction (Scholz, 1977). A major factor leading to the prediction was a long foreshock sequence: more than 500 of them were recorded within 4 days before the mainshock (Jones *et al.*, 1982). Wang *et al.* (2006) found that the role of foreshocks in this prediction was more psychological than scientific: the jolts and damage from increased seismicity in the preceding months worried earthquake workers and the general public, and the intensified foreshocks in the last day before the mainshock prompted some local officials to order an evacuation. In other places where official orders were not issued, the increased seismicity caused many residents to evacuate voluntarily.

The 1976 Tangshan earthquake (Ms 7.8)

The Great 1976 Tangshan earthquake occurred in the morning of July 28. The earthquake struck Tangshan, an industrial city 150 kilometers east of Beijing. In a brief moment, the earthquake destroyed the entire city and killed more than 242,000 people (Chen *et al.*, 1988). The maximum intensity reached XI in the epicentral region. An Ms 7.1 event followed 19 hours after the mainshock. The length of surface rupture produced by the mainshock is more than 47 km, and left-lateral slip is 1.5–2.3 m (Guo *et al*., 2011). The seismic moment released by the mainshock was 11.7×10^{19} N m.

The earthquake occurred within the broad fault system bounding the northern margin of the North China Plain. The hosting fault for the mainshock is a northeast-trending strike-slip faulting system with a dextral bend in the middle that divides the fault into the southern and northern segments (Nábělek *et al*., 1987; Shedlock *et al*., 1987).

5.6 Spatiotemporal patterns of large earthquakes

The spatiotemporal pattern of seismicity for a region is essential for hazard assessment. Establishing such a pattern, however, is difficult for most intracontinental regions because of the slow loading, infrequent large earthquakes, and incomplete earthquake records. The situation is better for North China – with its relatively frequent large earthquakes and long historic records, useful insight may be obtained.

5.6.1 Long-distance roaming of large earthquakes

Here we show the spatiotemporal occurrence of large earthquakes in North China during the past 700 years. For this relatively recent period, the catalog is likely complete for M $\geq$ 6 events (Huang *et al*., 1994) and it includes 49 M $\geq$ 6.5 events and at least four earthquakes of M $\geq$ 8, described in the previous section. Before the 1303 Hongdong earthquake, large earthquakes in North China were concentrated along the Weihe and Shanxi rifts and scattered over the North China Plain (Figure 5.7a). The Hongdong earthquake (M 8.0) occurred within the Shanxi rift, followed by the 1556 Huaxian earthquake (M 8.3) in the Weihe rift (Figure 5.7b). During this period, seismicity seemed to be concentrated within the Weihe–Shanxi rift systems, which would fit the model for rift zones to be the main host structures of intraplate earthquakes (Johnston and Kanter, 1990). However, the next large earthquake, the 1668 Tancheng earthquake (M 8.5), did not occur within the rift systems but more than 700 km to the east, on the Tanlu fault zone, which had little deformation through the late Cenozoic and only moderate previous seismicity. A decade later, another large event, the 1679 Sanhe earthquake (M 8.0), occurred only 40 km north of Beijing in a fault zone with limited previous seismicity and no clear surface exposure (Figure 5.7c). Then, in 1695, the Linfen earthquake (M 7.5–8.0) occurred in the Shanxi rift again, near the site of the 1303 Hongdong earthquake but on a different fault. Since then the Shanxi and Weihe rifts have been quiescent for more than 300 years, with only a few moderate earthquakes. Meanwhile, seismicity in the North China Plain apparently increased, producing three damaging earthquakes in the past century: the 1966 Xingtai earthquakes, the 1975 Haicheng earthquake, and the 1976 Tangshan earthquake (Figure 5.7d). These three large earthquakes were unexpected and occurred on previously unrecognized faults.

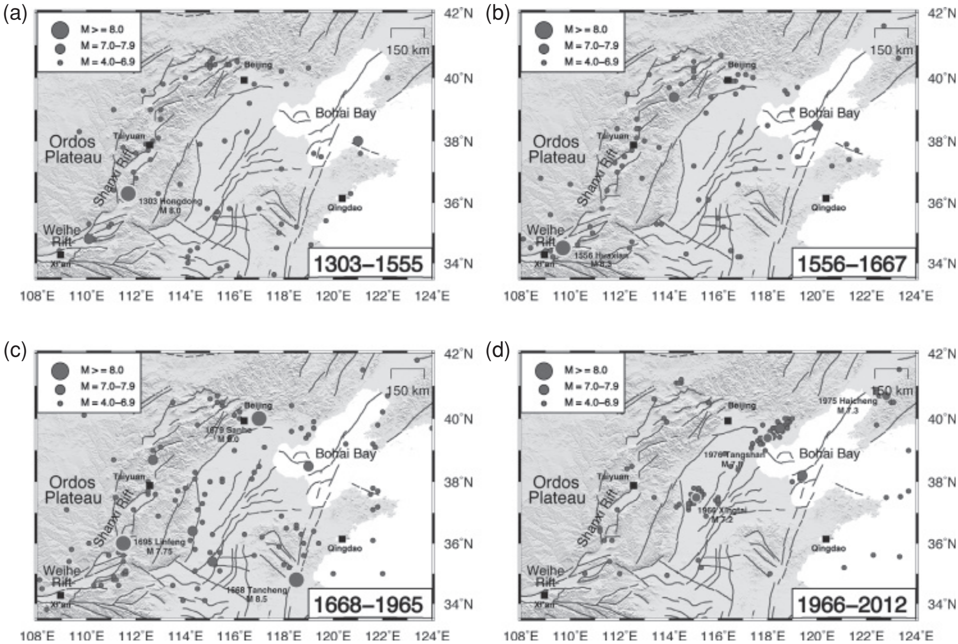

Figure 5.7 Spatiotemporal patterns of large earthquakes in North China in the past 700 years. The panels show earthquakes (epicenters indicated by dots) during various periods. Large dots with light rims are large earthquakes discussed in the text. After Liu *et al*. (2011).

5.6.2 Fault coupling and interaction

The spatiotemporal pattern of earthquakes in North China is much more complex than that at plate boundaries. Large earthquakes roamed between widespread fault systems. Is this roaming a random effect of long recurrence times on different faults? Or could these large earthquakes be related to each other through mechanical coupling and interaction between remote fault systems?

One approach is to study the stress links between these earthquakes. Wang *et al*. (1982) calculated the stress perturbations of the earthquake sequence in North China during the past 700 years and suggested that the subsequent events were linked to the previous ones. Shen *et al*. (2004) calculated the changes of Coulomb stress by the 48 M $\geq$ 6.5 events following the 1303 Hongdong earthquake, and concluded that 39 of them occurred in places where stress was elevated by previous earthquakes.

Another approach is to compare the seismic moment release on these fault systems. For a system of mechanically coupled fault zones, the total moment release rate should stay at a certain level, with the moment release rate of individual fault zones being complementary with each other (Dolan *et al*., 2007; Luo and Liu, 2012). Liu *et al*. (2011) showed that the moment release between the Weihe and Shanxi rifts seems to be complementary to each

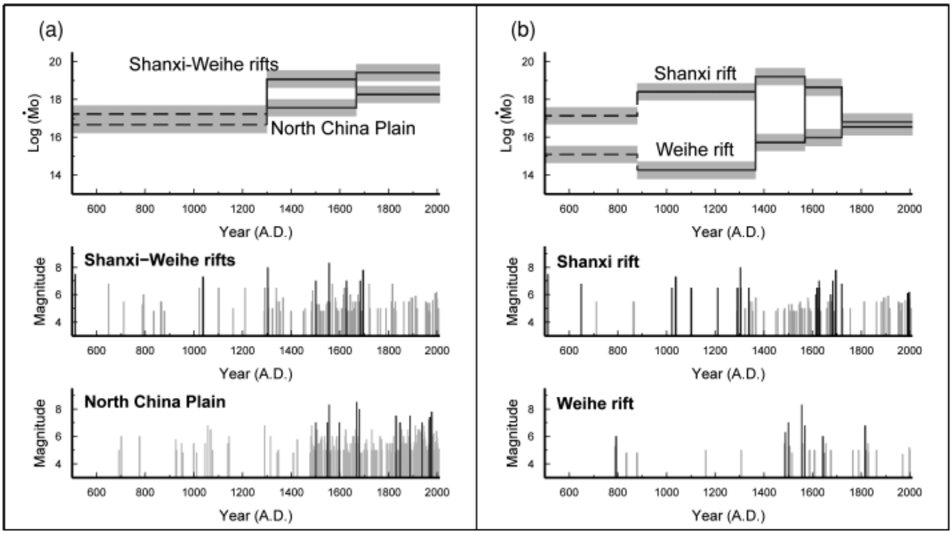

Figure 5.8 (a) Bottom two panels show occurrence and magnitude (M ≥ 4.0) of earthquakes in the North China Plain and the Shanxi–Weihe rifts. Top panel compares the time-averaged rate of seismic moment release (N m/yr) between them (tones are correlated with those in the bottom panels). Dashed lines are for older intervals, wherein some events are likely unrecorded. Gray bands indicate uncertainties associated with an estimated ±0.3 error in the magnitudes, which were based on the maximum intensity and the radius of the affected area (Ma, 1989). (b) Similar to (a) for the comparison of moment release between the Weihe and the Shanxi rifts. After Liu *et al.* (2011).

other, with increases in one corresponding to decreases in the other. Similar correlation exists between the Shanxi–Weihe rift system and the faults within the North China Plain (Figure 5.8). These results suggest that the fault systems in North China are mechanically coupled with each other.

5.6.3 A conceptual model for mid-continental earthquakes

These spatiotemporal patterns of earthquakes are not unique to North China; similar observations have been made in other mid-continents including Australia (Clark and McCue, 2003) and northwest Europe (Camelbeeck *et al.*, 2007). In the Central United States, the Meers fault in Oklahoma had a major earthquake about 1,200 years ago but is inactive today (Calais *et al.*, 2003). The New Madrid seismic zone, which has experienced several large earthquakes in the past few thousand years including at least three M ≥ 6.8 events in 1811–1812 (Johnston and Schweig, 1996; Tuttle *et al.*, 2002; Hough and Page, 2011), shows no significant surface deformation today (Calais and Stein, 2009) and its activity may be ending (Newman *et al.*, 1999; Calais and Stein, 2009; Stein and Liu, 2009).

The roaming of large earthquakes between widespread fault systems illustrates fundamental differences between earthquakes in mid-continents and at plate boundaries

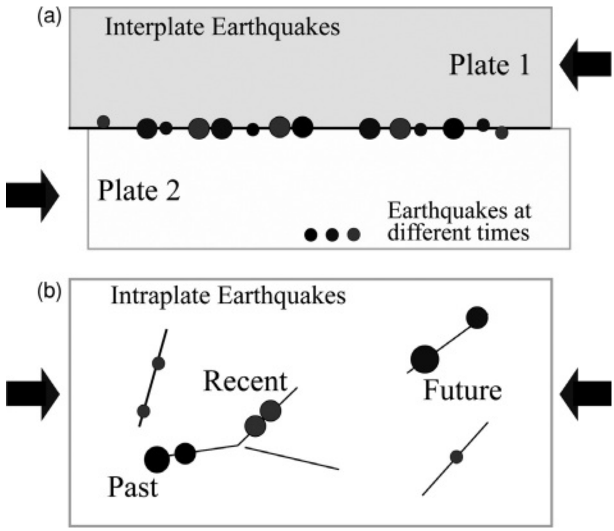

Figure 5.9 Conceptual models for the differences between interplate (a) and intraplate (b) earthquakes. For interplate earthquakes, the plate boundary fault is loaded at a constant rate by the steady relative plate motion, causing quasi-periodic earthquakes to concentrate along the plate boundary. In plate interiors, slow far-field tectonic loading is shared by a complex system of interacting faults. On each fault, the loading rate may be variable, and earthquakes may shut off on one fault and migrate to another.

(Figure 5.9). Plate boundary faults are loaded at constant rates by the steady relative plate motion. Consequently, earthquakes concentrate along the plate boundaries, and some quasi-periodic occurrences may be expected (Figure 5.9a), although the temporal patterns are often complicated (Jackson and Kagan, 2006). In contrast, in mid-continents the tectonic loading is shared by a complex system of interacting faults spread over a large region (Figure 5.9b), such that a large earthquake on one fault could affect the loading rates on remote faults (Li *et al.*, 2009). Because the slow tectonic loading is shared by many faults in mid-continents, individual faults may remain dormant for a long time and then become active for a short period, while seismicity moves to other faults.

5.7 Implications for earthquake hazards

The complex spatiotemporal patterns of earthquakes in North China pose serious challenges to the assessment of earthquake hazards. The current practice of hazard assessment is heavily influenced by the occurrence of previous large earthquakes (Figure 5.10), assuming that large earthquakes will be likely to repeat on the same faults. This line of reasoning can be traced back to Reid's elastic rebound theory (Reid, 1910), which implies cycles of energy accumulation and release on a given fault. However, the validity of this premise for intracontinental earthquakes has been questioned (Stein *et al.*, 2011, 2012). In North China,

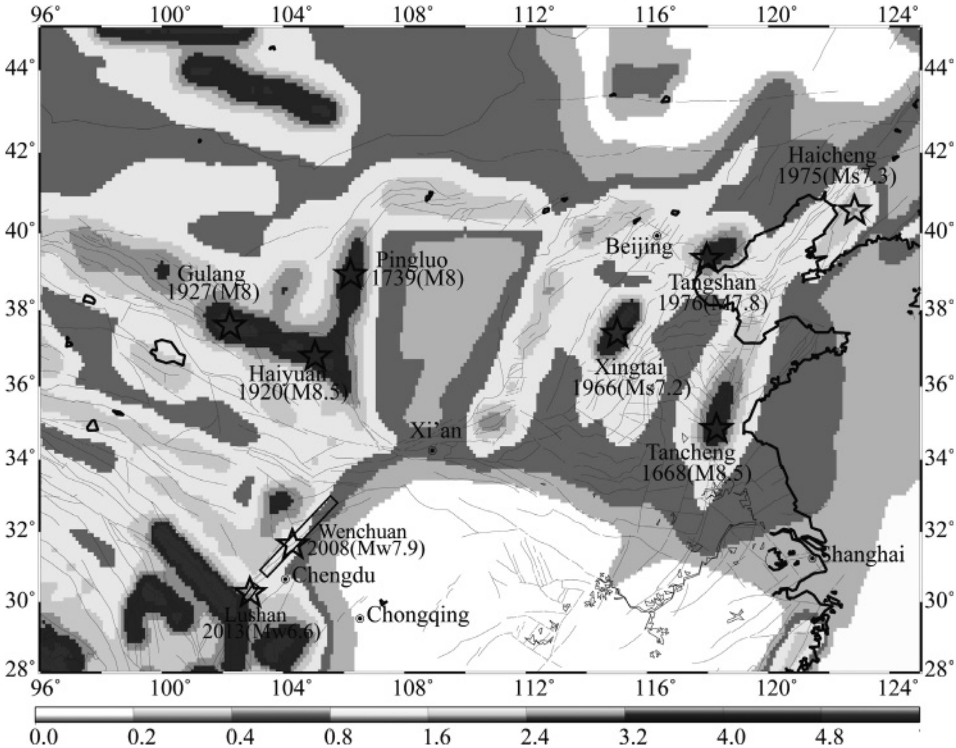

Figure 5.10 Seismic hazard map for North China and surrounding regions (GSHAP, 1999, http://www.seismo.ethz.ch/static/GSHAP). The hazard is expressed as the peak ground acceleration (PGA) on firm rocks, in m/s^2, expected to be exceeded in the next 50 years with a probability of 10%. The epicenters and rupture zones of the 2008 Wenchuan earthquake (Mw 7.9) and 2013 Lushan earthquakes (Mw 6.6) are indicated by stars and rectangles, respectively. For color version, see Plates section.

large earthquakes roamed between widespread fault systems; in the past 2,000 years, not a single M $\geq$ 7.0 earthquake ruptured the same fault segment twice. Such earthquake behavior raises questions about hazard maps such as that in Figure 5.10. Since the publication of this hazard map in 1999, a number of large earthquakes have occurred in this region, providing opportunities to test this assessment. Unfortunately, the map failed the test.

The devastating 2008 Wenchuan earthquake (Mw 7.9), which killed ~90,000 people, was not expected by the map maker (Figure 5.10). This earthquake ruptured the central and northern segments of the Longmenshan fault, which was assigned a moderate to low risk by the hazard map, presumably because of the low fault slip rates (<3 mm/yr) and the lack of large earthquakes in the past few centuries. The high risk zones on the map are where large earthquakes occurred in the recent past, such as along the Xianshuihe fault. Five years after the Wenchuan earthquake, the 2013 Lushan earthquake (Mw 6.6) ruptured the southern segment of the Longmenshan fault, also assigned with moderate to low risk on the hazard map (Figure 5.10). The Wenchuan and Lushan earthquakes show clearly that having no previous large earthquakes does not mean having no future large earthquakes.

Within North China, the hazard map assigns the highest risk to the Tangshan, Xingtai, and Tancheng regions, apparently because of the 1966 Xingtai and the 1976 Tangshan earthquakes, and because of the big Tancheng earthquake (M 8.5) in 1668. The Shanxi rift zone was assigned with lower risk, presumably because it has been seismically quiescent for the past 300 years. The Weihe rift zone was assigned a low risk because the 1556 Huaxian earthquake (M 8.0) was the last large earthquake within the rift.

The nearly 3,000 years of earthquake records in North China, however, indicate an earthquake behavior more complicated than that assumed in the current practice of hazard assessment. Because the large earthquakes tend to roam between widespread fault systems, previous large earthquakes may not be a good indicator of where a future large earthquake will occur; because strain can accumulate in the fault zones for thousands of years before being released by a large earthquake, low slip rates do not mean being safe; and not having previous large earthquakes does not mean no large earthquakes in the future. And finally, because it usually take thousands of years for intracontinental fault zones to accumulate enough strain energy for a large earthquake, places where large earthquakes occurred in the recent past are not necessarily more dangerous than other places.

Another challenge for earthquake hazard assessment in North China, and in other mid-continents, is the long sequences of aftershocks (Stein and Liu, 2009). Small earthquakes are often regarded as signs of stress building up towards the next big earthquake; their occurrence in source regions of previous large earthquakes therefore often causes alarm. One example is the recent sequence of moderate sized earthquakes in the Tangshan region, which includes an M 4.8 event on May 28 and an M 4.0 event on June 18, 2012. These earthquakes caused widespread concerns and heated debate in China: are they aftershocks of the great 1976 Tangshan earthquake, or are they harbingers of a new period of active seismicity in Tangshan and the rest of North China, where seismic activity seems fluctuate between highs and lows over periods of a few decades (Ma, 1989)?

Liu and Wang (2012) showed that this recent seismicity in Tangshan is likely the aftershocks of the 1976 Tangshan earthquake for the following reasons: (1) The seismicity rate in the Tangshan region has been decaying since 1976, following Omori's law, but is still clearly above the background level (Figure 5.11). (2) The seismicity rates of the Tangshan, Xingtai, and Haicheng regions for 1986–2010 (i.e., 10 years after the Tangshan earthquake and 20 years after the Xingtai earthquake) are clearly higher than the average value for the North China Plain. This indicates either that these regions are tectonically more active than the rest of the North China Plain, or the continuing influence of aftershocks of the large earthquakes decades ago. Because these regions showed no sign of abnormal tectonic activity before the large earthquakes, aftershocks are more likely the cause. (3) Strain rates calculated from GPS data are higher in the Tangshan and Xingtai regions than that of the

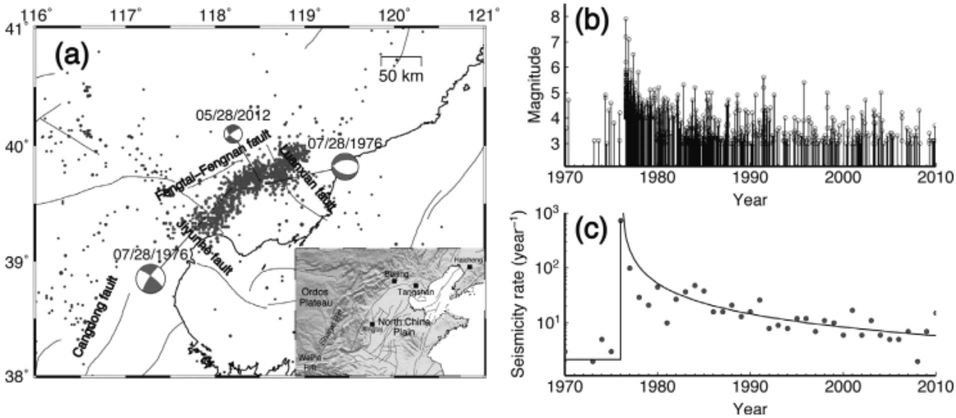

Figure 5.11 (a) Seismicity in the source region of the 1976 Tangshan earthquake. Dots are epicenters of aftershocks; circles are background seismicity (M ≥ 3.0, 1970–2011). The focal mechanism solutions are for the two mainshocks of 1976 and the May 5, 2012 event. The inset map shows the location of the Tangshan region. (b) Earthquake sequence in the source region of the great Tangshan earthquake since 1970. (c) Seismicity rates (number of events per year) of the Tangshan earthquake sequence. Solid lines are least-square fitting.

rest of the North China Plain. Again, because these regions have no evidence of unusually high tectonic activity relative to other fault zones in the North China Plain, the higher strain rates indicate that postseismic deformation continues to the present (the Haicheng region does not have sufficient GPS stations to allow a meaningful strain calculation).

The long-distance roaming of large earthquakes and their long sequences of aftershocks hence make seismic hazard assessment, a challenging task for any region (Stein *et al.*, 2011, 2012), more difficult in North China and other mid-continents. If the earthquakes roam between widespread faults, the current practice, which uses previous large earthquakes as hints to locate future earthquakes, tends to overestimate the hazard in places where previous large earthquakes occurred, and underestimate the hazard elsewhere. And if the aftershock sequences last a long time, small aftershocks may be misread as precursors.

This situation cannot be fundamentally improved by simply extending the earthquake records alone. This is because earthquakes in North China and other mid-continents do not fit the model of well-identified faults being steadily loaded. Instead, these earthquakes are the products of widespread faults interacting with each other in a complex dynamic system (Stein *et al.*, 2009). Hence, we cannot treat each individual fault or fault segment as an isolated system and expect some regular recurrence time. In a complex system where changes of any part have nonlinear impacts on all other parts (Stein *et al.*, 2009), the concepts of stress cycles, characteristic earthquakes, and recurrence time may not hold – their validity has been questioned even for interplate earthquakes (Jackson and Kagan, 2006). Recognizing the fault systems in North China and other mid-continents as complex dynamic systems does not make hazard assessment easier, but it would be a necessary paradigm shift. Geodynamic modeling will need to explore how faults interact over long distances and multiple timescales (e.g., Luo and Liu, 2012), rather than focusing on stress evolution on an isolated fault or fault segment. Paleoseismic studies should not be limited to where large earthquakes occurred recently, and detailed and careful analysis are needed to determine the age and spatial scale of past events, without trying to fit expected recurrence intervals (Xu and Deng, 1996). As for North China, the potential for repeated large earthquakes in Tangshan and Xingtai is likely lower than that generally perceived, if the 2,000-year historic record can provide any hints. In contrast, the Shanxi rift zone, which has produced more than 36 M ≥ 6.5 earthquakes since 1303 but has been quiescent for the past 300 years, may deserve closer monitoring, and the Weihe rift zone, the host for the 1556 Huaxian earthquake (M 8.0) and with relatively high contemporary strain rates (Figure 5.5a), may not be as safe as suggested by the hazard map.

Acknowledgements

Seth Stein inspired our interest in intraplate earthquakes and co-authored a number of papers reviewed here. We thank Roy Van Arsdale and Pradeep Talwani for their constructive reviews. ML's research in China is supported by NSF/OISE grant 0730154 and a grant from the Chinese Academy of Sciences. HW acknowledges support from the National Natural Science Foundation of China (Grants 41104058 and 41104057).

References

Allen, M. B., D. I. M. Macdonald, Z. Xun, S. J. Vincent, and M. C. Brouet (1998). Transtensional deformation in the evolution of the Bohai Basin, northern China. In *Continental Transpressional and Transtensional Tectonics*, ed. R. E. Holdsworth, R. A. Strachan, and J. F. Dewey. Geological Society, London, Special Publication, 135 215–229.

Bi, L., H. He, Y. Xu, Z. Wei, and F. Shi (2011). The extraction of knickpoint series based on the high resolution DEM data and the identification of paleoearthquakes: a case study of the Huoshan Mts. Piedmont fault (in Chinese with English abstract). *Seismology and Geology*, 33(04), 963–977.

Bryant, D. L., J. C. Ayers, S. Gao, C. F. Miller, and H. Zhang (2004). Geochemical, age, and isotopic constraints on the location of the Sino–Korean/Yangtze Suture and evolution of the Northern Dabie Complex, east central China. *Geological Society of America Bulletin*, 116(5–6), 698–717.

Calais, E., and S. Stein (2009). Time-variable deformation in the New Madrid Seismic Zone. *Science*, 323(5920), 1442.

Calais, E., M. Vergnolle, V. San'kov, *et al*. (2003). GPS measurements of crustal deformation in the Baikal-Mongolia area (1994–2002): implications for current kinematics of Asia. *Journal of Geophysical Research, Solid Earth*, 108(B10), 2501.

Camelbeeck, T., K. Vanneste, P. Alexandre, *et al*. (2007). Relevance of active faulting and seismicity studies to assess long term earthquake activity in Northwest Europe. In *Continental Intraplate Earthquakes: Science, Hazard, and Policy Issues*, ed. S. Stein, and S. Mazzotti. Geological Society of America Special Paper 425, pp. 193–224.

Chen, L., C. Cheng, and Z. Wei (2009). Seismic evidence for significant lateral variations in lithospheric thickness beneath the central and western North China Craton. *Earth and Planetary Science Letters*, 286(1–2), 171–183.

Chen, Y., B. Lin, Z. Lin, and Z.-Y. Li (1975). The focal mechanism of the 1966 Xingtai earthquake as inferred from the ground deformation observations. *Acta Geophysica Sinica*, 18(3), 164–182.

Chen, Y., K. L. Tsoi, F. B. Chen, *et al*. (1988). *The Great Tangshan Earthquake of 1976: An Anatomy of Disaster*. Oxford: Pergamon Press.

Cheng, X., Z. Su, and W. An (1995). Tectonic background of the big Linfen earthquake in 1695. *Earthquake Research in Shanxi* (in Chinese with English Abstract), Z1, 43–48.

Chung, W.-Y., and J. J. Cipar (1983). Source modeling of the Hsingtai, China earthquakes of March 1966. *Physics of the Earth and Planetary Interiors*, 33(2), 111–125.

Clark, D., and K. McCue (2003). Australian paleoseismology: towards a better basis for seismic hazard estimation. *Annals of Geophysics*, 46(5), 1087–1106.

Deng, Q., and Y. Liao (1996). Paleoseismology along the range-front fault of Helan Mountains, north central China. *Journal of Geophysical Research: Solid Earth*, 101(B3), 5873–5893.

Deng, Q. D., P. Z. Zhang, Y. K. Ran, *et al*. (2002). Basics characteristics of active tectonics of China (in Chinese). *Science in China (Series D)*, 32(12), 1020–1030.

Deng, Q., P. Zhang, Y. Ran, *et al*. (2003). Basic characteristics of active tectonics of China. *Science in China Series D: Earth Sciences*, 46(4), 356–372.

Dolan, J. F., D. D. Bowman, and C. G. Sammis (2007). Long-range and long-term fault interactions in Southern California. *Geology*, 35(9), 855–858.

Griffin, W. L., A. Zhang, S. Y. O'Reilly, and C. G. Ryan (1998). Phanerozoic evolution of the lithosphere beneath the Sino-Korean Craton. In *Mantle Dynamics and Plate Interactions in East Asia*, ed. M. F. J. Flower, S.-L. Chung, C.-H. Lo, and T.-Y. Lee. Washington, DC: American Geophysical Union, pp. 107–126.

Gu, G. X., T. H. Lin, Z. L. Shi, and Q. Li (1983). *Earthquake Catalog of China: 1831 B.C. – 1969 A.D. (in Chinese)*. Beijing: Science Publishing House.

Guo, H., W. Jiang, and X. Xie (2011). Late-Quaternary strong earthquakes on the seismogenic fault of the 1976 Ms 7.8 Tangshan earthquake, Hebei, as revealed by drilling and trenching. *Science in China Series D-Earth Sciences*, 41(7), 1009–1028.

Guo, H., W. Jiang, and X. Xie (2012). Analysis of Holocene faulting phenomena revealed in the three trenches along the northern and central Jiaocheng fault, Shanxi. *Seismology and Geology (in Chinese with English abstract)*, (01), 76–92.

He, J., M. Liu, and Y. Li (2003). Is the Shanxi rift of northern China extending? *Geophysical Research Letters*, 30, doi:10.1029/2003GL018764.

Hough, S., and M. Page (2011). Toward a consistent model for strain accrual and release for the New Madrid Seismic Zone, central United States. *Journal of Geophysical Research*, 116, doi:10.1029/2010JB007783.

Hu, X., G. Diao, J. Gao, *et al*. (2002). Application of present small earthquakes to infer the focal faults of two large historical earthquakes in Hongdong and Linfen, Shanxi Province. *Earthquake Research in China*, 18(1), 76–85.

Huan, W., Z. Shi, and S. Li (2003). The new evidence for epicenter location and seismogenic structure of the 1556 M 8 1/4 large earthquake. *Earthquake Research in China*, 19(01), 20–32.

Huang, J. L., and D. P. Zhao (2006). High-resolution mantle tomography of China and surrounding regions. *Journal of Geophysical Research, Solid Earth*, 111, B09305, doi:10.1029/2005JB004066.

Huang, W. Q., W. X. Li, and X. F. Cao (1994). Research on the completeness of earthquake data in the Chinese mainland (II). *Acta Seismologica Sinica*, 16(4), 423–432.

Huang, Z., H. Li, Y. Zheng, and Y. Peng (2009). The lithosphere of North China Craton from surface wave tomography. *Earth and Planetary Science Letters*, 288(1–2), 164–173.

Jackson, D. D., and Y. Y. Kagan (2006). The 2004 Parkfield earthquake, the 1985 prediction, and characteristic earthquakes: lessons for the future. *Bulletin of the Seismological Society of America*, 96(4B), S397–409.

Jiang, W., Z. Hou, Z. Xiao, and X. Xie (2000). Study on paleoearthquakes of Qixinzhuang trench at the Xiadian fault, Beijing plain (in Chinese with English abstract). *Seismology and Geology*, 04, 413–422.

Johnston, A. C., and L. R. Kanter (1990). Earthquakes in stable continental crust. *Scientific American*, 262(3), 68–75.

Johnston, A. C., and E. S. Schweig (1996). The enigma of the New Madrid earthquakes of 1811–1812. *Annual Review of Earth and Planetary Sciences*, 24, 339–384.

Jones, L. M., B. Wang, S. Xu, and T. J. Fitch (1982). The foreshock sequence of the February 4, 1976, Haicheng earthquake ($M = 7.3$). *Journal of Geophysical Research, Solid Earth*, 87(B6), 4575–4584.

Li, Q., M. Liu, and S. Stein (2009). Spatial-temporal complexity of continental intraplate seismicity: insights from geodynamic modeling and implications for seismic hazard estimation. *Bulletin of the Seismological Society of America*, 99(1), doi: 10.1785/0120080005.

Li, S. (1981). *Earthquakes in China*. Beijing: Seismological Press.

Li, S., G. Zhao, L. Dai, *et al*. (2012). Cenozoic faulting of the Bohai Bay Basin and its bearing on the destruction of the eastern North China Craton. *Journal of Asian Earth Sciences*, 47(0), 80–93.

Li, Z.-X. (1994). Collision between the North and South China blocks: a crustal-detachment model for suturing in the region east of the Tanlu fault. *Geology*, 22(8), 739–742.

Lin, W., and W. Gao (1987). The occurrence intervals of large earthquakes in the Yishu fault zone (in Chinese). *China Earthquakes*, 03, 36–42.

Liu, D. Y., A. P. Nutman, W. Compston, J. S. Wu, and Q. H. Shen (1992). Remnants of ≥3800 Ma crust in the Chinese part of the Sino-Korean craton. *Geology*, 20(4), 339–342.

Liu, M., and H. Wang (2012). Roaming earthquakes in China highlight midcontinental hazards. *Eos, Transactions, American Geophysical Union*, 93(45), 453–454.

Liu, M., and Y. Yang (2005). Contrasting seismicity between the North China and South China blocks: kinematics and geodynamics. *Geophysical Research Letters*, 32 (L12310), doi:10.1029/2005GL023048.

Liu, M., X. Cui, and F. Liu (2004). Cenozoic rifting and volcanism in eastern China: a mantle dynamic link to the Indo-Asian collision? *Tectonophysics*, 393, 29–42.

Liu, M., Y. Yang, Z. Shen, *et al*. (2007). Active tectonics and intracontinental earthquakes in China: the kinematics and geodynamics. In *Continental Intraplate Earthquakes:*

Science, Hazard, and Policy Issues, ed. S. Stein, and S. Mazzotti. Geological Society of America Special Paper 425, pp. 209–318, doi: 210.1130/2007.2425.

Liu, M., S. Stein, and H. Wang (2011). 2000 years of migrating earthquakes in North China: how earthquakes in midcontinents differ from those at plate boundaries. *Lithosphere*, 3, 128–132.

Luo, G., and M. Liu (2012). Multi-timescale mechanical coupling between the San Jacinto Fault and the San Andreas Fault, southern California. *Lithosphere*, doi: 10.1130/L1180.1131.

Ma, X. (1989). *Lithospheric Dynamics Altas of China*. Beijing: China Cartographic Publishing House.

Ma, Y., and P. Zhong (2009). Summary of the M8 1/2 Tancheng earthquake in 1668 (in Chinese). *Recent Developments in World Seismology*, 2, 9–18.

Menzies, M. A., and Y. Xu (1988). Geodynamics of the North China Craton. In *Mantle Dynamics and Plate Interactions in East Asia*, ed. M. F. J. Flower, S. L. Chung, C. H. Lo, and T. Y. Lee. Washington, DC: American Geophysical Union, 27, 155–165.

Menzies, M., Y. G. Xu, H. F. Zhang, and W. M. Fan (2007). Integration of geology, geophysics and geochemistry: a key to understanding the North China Craton. *Lithos*, 96(1–2), 1–21.

Min, Z., G. Wu, Z. Jiang, C. Liu, and Y. Yang (1995). *The Catalog of Chinese Historic Strong Earthquakes (B.C. 23–AD 1911)* (in Chinese). Beijing: Seismological Publishing House.

Mooney, W. D., J. Ritsema, and Y. K. Hwang (2012). Crustal seismicity and the earthquake catalog maximum moment magnitude (Mc_{max}) in stable continental regions (SCRs): correlation with the seismic velocity of the lithosphere. *Earth and Planetary Science Letters*, 357–358, 78–83.

Nábělek, J., W.-P. Chen, and H. Ye (1987). The Tangshan earthquake sequence and its implications for the evolution of the North China Basin. *Journal of Geophysical Research*, 92(B12), 12615–12628.

Newman, A., S. Stein, J. Weber, *et al*. (1999). Slow deformation and lower seismic hazard at the New Madrid Seismic Zone. *Science*, 284(5414), 619–621.

Ran, Y., Q. Deng, X. Yang, *et al*. (1997). Paleoearthquakes and recurrence interval on the seismogenic fault of 1679 Sanhe-pinggu M8 earthquake, Hebei and Beijing. *Seismology and Geology*, 19(3), 193–201.

Ran, Y., L. Chen, X. Yang, and Z. Han (2003a). Recurrence characteristics of late-quaternary strong earthquakes on the major active faults along the northern border of Ordos block. *Science in China Series D, Earth Sciences*, 46, 189–200.

Ran, Y., P. Zhang, and L. Chen (2003b). Late Quaternary history of paleoseismic activity along the Hohhot Segment of the Daqingshan piedmont fault in Hetao depression zone, North China. *Annals of Geophysics*, 46, 1053–1069.

Reid, H. F. (1910). *The Mechanics of the Earthquake, The California Earthquake of April 18, 1906*, Report of the State Investigation Commission Vol. 2.

Ren, J., K. Tamaki, S. Li, and J. Zhang (2002). Late Mesozoic and Cenozoic rifting and its dynamic setting in Eastern China and adjacent areas. *Tectonophysics*, 344(3–4), 175–205.

Scholz, C. H. (1977). A physical interpretation of the Haicheng earthquake prediction. *Nature*, 267, 121–124.

Seismological Bureau of Hebei Province (1986). *The 1966 Xingtai Earthquake*. Beijing: China Seismological Press.

Shedlock, K. M., J. Baranowski, X. Weiwen, and H. X. Liang (1987). The Tangshan aftershock sequence. *Journal of Geophysical Research*, 92(B3), 2791–2803.

Shen, Z. K., C. Zhao, A. Yin, and D. Jackson (2000). Contemporary crustal deformation in east Asia constrained by Global Positioning System measurements. *Journal of Geophysical Research*, 105, 5721–5734.

Shen, Z. K., Y. Wan, W. Gan, T. Li, and Y. Zeng (2004). Crustal stress evolution of the last 700 years in North China and earthquake sequence (in Chinese). *Earthquake Research in China*, 20, 211–228.

Stein, S., and M. Liu (2009). Long aftershock sequences within continents and implications for earthquake hazard assessment. *Nature*, 462(7269), 87–89.

Stein, S., M. Liu, E. Calais, and Q. Li (2009). Mid-Continent earthquakes as a complex system. *Seismological Research Letters*, 80(4), 551–553.

Stein, S., R. Geller, and M. Liu (2011). Bad assumptions or bad luck: why earthquake hazard maps need objective testing. *Seismological Research Letters*, 82(5), 623–626.

Stein, S., R. J. Geller, and M. Liu (2012). Why earthquake hazard maps often fail and what to do about it. *Tectonophysics*, 562–563, 1–25.

Su, Z., Z. Yuan, and J. Zhao (2003). A review on studies concerned with the 1303 Hongtong earthquake (in Chinese with English abstract). *Earthquake Research in Shanxi*, 03, 4–22.

The Geodetic Survey Brigade for Earthquake Research, N.S.B. (1975). Crustal deformation associated with the Hsingtai earthquake in March, 1966. *Chinese Journal of Geophysics, Chinese Edition*, 18(3), 153–163.

Tuttle, M. P., E. S. Schweig, J. D. Sims, *et al*. (2002). The earthquake potential of the New Madrid seismic zone. *Bulletin of the Seismological Society of America*, 92(6), 2080–2089.

Wang, H., and J. Geng (1996). Discussion about hypocenter parameters of the M8.5 Tancheng earthquake in 1668 (in Chinese). *Journal of Seismology*, 4, 29–35.

Wang, H., M. Liu, J. Cao, X. Shen, and G. Zhang (2011). Slip rates and seismic moment deficits on major active faults in mainland China. *Journal of Geophysical Research*, 116, B02405, doi:02410.01029/02010JB007821.

Wang, K., Q. Chen, S. Sun, and A. Wang (2006). Predicting the 1975 Haicheng earthquake. *Bulletin of the Seismological Society of America*, 96(3), 757–795.

Wang, R., S. Y. Sun, and Y. G. Cai (1982). Numerical simulation of earthquake sequences in North China over the past 700 years (in Chinese). *Science in China, B*, 8(745–753).

Wesnousky, S. G., L. M. Jones, C. H. Scholz, and Q. Deng (1984). Historical seismicity and rates of crustal deformation along the margins of the Ordos block, North China. *Bulletin of the Seismological Society of America*, 74, 1767–1783.

Wu, L., S. Qi, and R. Wang (1988). The 1303 Hongton earthquake of M = 8 and the 1695 Linfen earthquake M = 8 in Shanxi Province. In *China Special Large Earthquakes Research* (in Chinese), ed. Z.-J. Guo and Z.-J. Ma. Beijing: Seismological Press, pp. 6–35

Xie, X., W. Jiang, R. Wang, H. Wang, and X. Feng (2003). Holocene paleo-seismic activities on the Kouquan fault zone, Datong basin, Shanxi Province (in Chinese with English abstract). *Seismology and Geology* 03, 359–374.

Xu, C., L. Dong, C. Shi, Y. Li, and X. Hu (2002a). A study on annual accumulation of strain energy density significance by using GPS measurements in North China (in Chinese with English abstract). *Chinese Journal of Geophysics, Chinese Edition*, 45(4), 497–506.

Xu, J., Z. Fang, and L. Yang (1988a). Tectonic background and causative fault of 1966 Xingtai Ms7.2 earthquake (in Chinese). *Seismology and Geology*, 10(4), 51–59.

Xu, X., and Q. Deng (1990). The features of Late Quaternary activity of the piedmont fault of Mt. Huoshan, Shanxi Province and the 1303 Hongtong earthquake (M = 8) (in Chinese). *Seismology and Geology*, 12(1), 21–30.

Xu, X., and Q. Deng (1996). Nonlinear characteristics of paleoseismicity in China. *Journal of Geophysical Research, Solid Earth*, 101(B3), 6209–6231.

Xu, X., H. Zhang, and Q. Deng (1988b). The paleoearthquake traces on Huashan front fault zone in Weihe basin and its earthquake intervals (in Chinese with English abstract). *Seismology and Geology*, 04, 206.

Xu, X., X. Ma, and Q. Deng (1993). Neotectonic activity along the Shanxi rift system, China. *Tectonophysics*, 219(4), 305–325.

Xu, X. W., W. M. Wu, X. K. Zhang, *et al*. (2002b). *Neotectonics and Earthquakes in the Capital Circle Region*. Beijing: Science Press.

Xu, Y. G. (2001). Thermo-tectonic destruction of the archaean lithospheric keel beneath the Sino-Korean craton in China: evidence, timing and mechanism. *Physics and Chemistry of the Earth, Part A: Solid Earth and Geodesy*, 26(9–10), 747–757.

Xu, Y. G., M. A. Menzies, M. F. Thirlwall, *et al*. (2003). “Reactive” harzburgites from Huinan, NE China: products of the lithosphere-asthenosphere interaction during lithospheric thinning? *Geochimica et Cosmochimica Acta*, 67, 487–505.

Yao, G., Y. Jiang, and X. Yu (1984). Investigation on the 1303 Zhaocheng, Shanxi, earthquake (M = 8) and its parameters concerned (in Chinese with English abstract). *Journal of Seismological Research*, 7(13), 313–326.

Ye, H., B. Zhang, and F. Mao (1987). The Cenozoic tectonic evolution of the Great North China: two types of rifting and crustal necking in the Great North China and their tectonic implications. *Tectonophysics*, 133, 217–227.

Yin, A., and S. Nie (1996). Phanerozoic palinspastic reconstruction of China and its neighbouring regions. In *Tectonic Evolution of Aisa*, ed. A. Yin and M. Harrison. New York: Cambridge University Press, Rubey Volume IX, pp. 442–485.

Zhai, M.-G., and M. Santosh (2011). The early Precambrian odyssey of the North China Craton: a synoptic overview. *Gondwana Research*, 20(1), 6–25.

Zhang, P., and W. Gan (2008). Combined model of rigid-block motion with continuous deformation: patterns of present-day deformation in continental China. In *Investigations into the Tectonics of the Tibetan Plateau*, ed. B. C. Burchfiel and E. Wang, Geological Society of America Special Paper 444, pp. 59–71, doi:10.1130/2008.2444(1104).

Zhang, Y., J. L. Mercier, and P. Vergely (1998). Extension in the graben systems around the Ordos (China), and its contribution to the extrusion tectonics of south China with respect to Cobi-Mongolia. *Tectonophysics*, 285, 41–75.

Zhang, Y., Y. Ma, N. Yang, W. Shi, and S. Dong (2003). Cenozoic extensional stress evolution in North China. *Geodynamics*, 36, 591–613.

Zhang, Y., C. Liao, W. Shi, T. Zhang, and F. Guo (2007). Jurassic deformation in and around the Ordos Basin, North China. *Earth Science Frontiers*, 14(2), 182–196.

Zhao, G., M. Sun, S. A. Wilde, and L. Sanzhong (2005). Late Archean to Paleoproterozoic evolution of the North China Craton: key issues revisited. *Precambrian Research*, 136(2), 177–202.

Zhu, F., and G. Wu (1982). *The 1975 Haicheng Earthquake*. Beijing: China Seismological Press.

Zhu, G. Z., Y. L. Shi, S. Chen, and H. Zhang (2009). Numerical simulations on deep subduction of western pacific plate to NE China. *Chinese Journal of Geophysics (Acta Geophysica Sinica)*, 52(4), 950–957.

Zhu, R. X., Y. G. Xu, G. Zhu, *et al*. (2012a). Destruction of the North China Craton. *Science China, Earth Sciences*, 55(10), 1565–1587.

Zhu, R. X., J. H. Yang, and F. Y. Wu (2012b). Timing of destruction of the North China Craton. *Lithos*, 149, 51–60.